Contact
Volume 6: 1–6

DOI: 10.1177/25152564231183897
journals.sagepub.com/home/ctc

Stranger Twins: A Tale of Resemblance and Contrast Between VAP Proteins

Mélody Subra, Zoé Grimanelli, Romain Gautier, and Bruno Mesmin

Abstract

When considering the vesicle-associated membrane protein-associated protein (VAP) family, major receptors at the surface of the endoplasmic reticulum (ER), it appears that VAP-A and VAP-B paralogs largely overlap in structure and function, and that specific features to distinguish these two proteins hardly exist or are poorly documented. Here, we question the degree of redundancy between VAP-A and VAP-B: is one simply a backup plan, in case of loss of function of one of the two genes, or are there molecular and functional divergences that would explain their maintenance during evolution?

Keywords

endoplasmic reticulum, VAP, membrane contact sites, tether, structural biology

Vesicle-associated membrane protein-associated protein (VAP): VAP-A and VAP-B are ubiquitously expressed type-II endoplasmic reticulum (ER) transmembrane (TM) proteins, with homologs widely distributed from yeast to human, involved in several functions at membrane contact sites (MCS), and implicated in genetic and infectious diseases (Murphy and Levine, 2016; Neefjes and Cabukusta, 2021; Kors et al., 2022). They encompass a N-terminal major sperm protein (MSP) domain, a central coiled-coil region for dimerization and a C-terminal TM domain (Figure 1A). Two intrinsically disordered regions (linkers 1 and 2) connect these different domains together and ensure VAP flexibility (Subra et al., 2023). VAP-A and VAP-B act as receptors for ~100 proteins containing a short recognition motif called "two phenylalanines in an acidic tract" (FFAT), which consists of the consensus sequence EFFDAxE flanked by acidic residues (Loewen et al., 2003). VAP-A and VAP-B share 63% sequence identity and 83% similarity. Their MSP domain, responsible for FFAT binding, are nearly identical (82% sequence identity) and highly conserved. The FFAT motif binding site within the MSP is positively charged and includes two residues (K94 and M96 in VAP-A and K87 and M89 in VAP-B) that are key for VAP-FFAT interaction (Kaiser et al., 2005). VAP proteins tolerate many variations in the FFAT sequence, and also bind phospho-FFAT (pFFAT) motifs, which must be phosphorylated to interact with the MSP (Di Mattia et al., 2020). For example, STARD3, MIGA2, PTPIP51, and the voltage-gated membrane potassium channels Kv2.1 and Kv2.2 encompass a pFFAT (Alpy et al., 2013; Sun and De Camilli, 2018; Xu et al., 2020; Yeo et al., 2021). Amino acid variations within FFAT motifs may influence affinities between VAP-A or VAP-B and their partners, and thus modulate their respective subcellular localization.

Despite their high sequence similarity, a few genetic mutations are known to affect VAP-B but not VAP-A, including the prevalent VAP-B P56S mutation in its MSP domain, which is linked to a rare dominantly inherited form of amyotrophic lateral sclerosis (ALS-8) (Nishimura et al., 2004). The P56S mutation leads to MSP misfolding, resulting in the formation of aggregates, which are ubiquitinated and eliminated (Borgese et al., 2021). Curiously, proline 56 is conserved in VAP-A, but incorporating the same mutation in VAP-A causes minor effects. It appears that VAP-A is resistant to aggregation because it contains three prolines in a highly conserved sequence of its MSP, called the VAP Consensus Sequence (VCS; aa. 42–63), whereas VAP-B has only two prolines in its VCS. Mutation of a second proline in VAP-A VCS leads to massive aggregation resembling the VAP-B P56S phenotype (Nakamichi et al., 2011). However, this does not appear to be a strict requirement, as the *Drosophila* protein contains three prolines in the same region, yet the ALS-8-causing mutation

Institut de Pharmacologie Moléculaire et Cellulaire, Inserm, CNRS, Université Côte d'Azur, Valbonne, France

Received May 2, 2023; Accepted June 6, 2023

Corresponding Author:
Bruno Mesmin, Institut de Pharmacologie Moléculaire et Cellulaire, Inserm, CNRS, Université Côte d'Azur, 660 route des lucioles, 06560 Valbonne, France.
Email: mesmin@ipmc.cnrs.fr

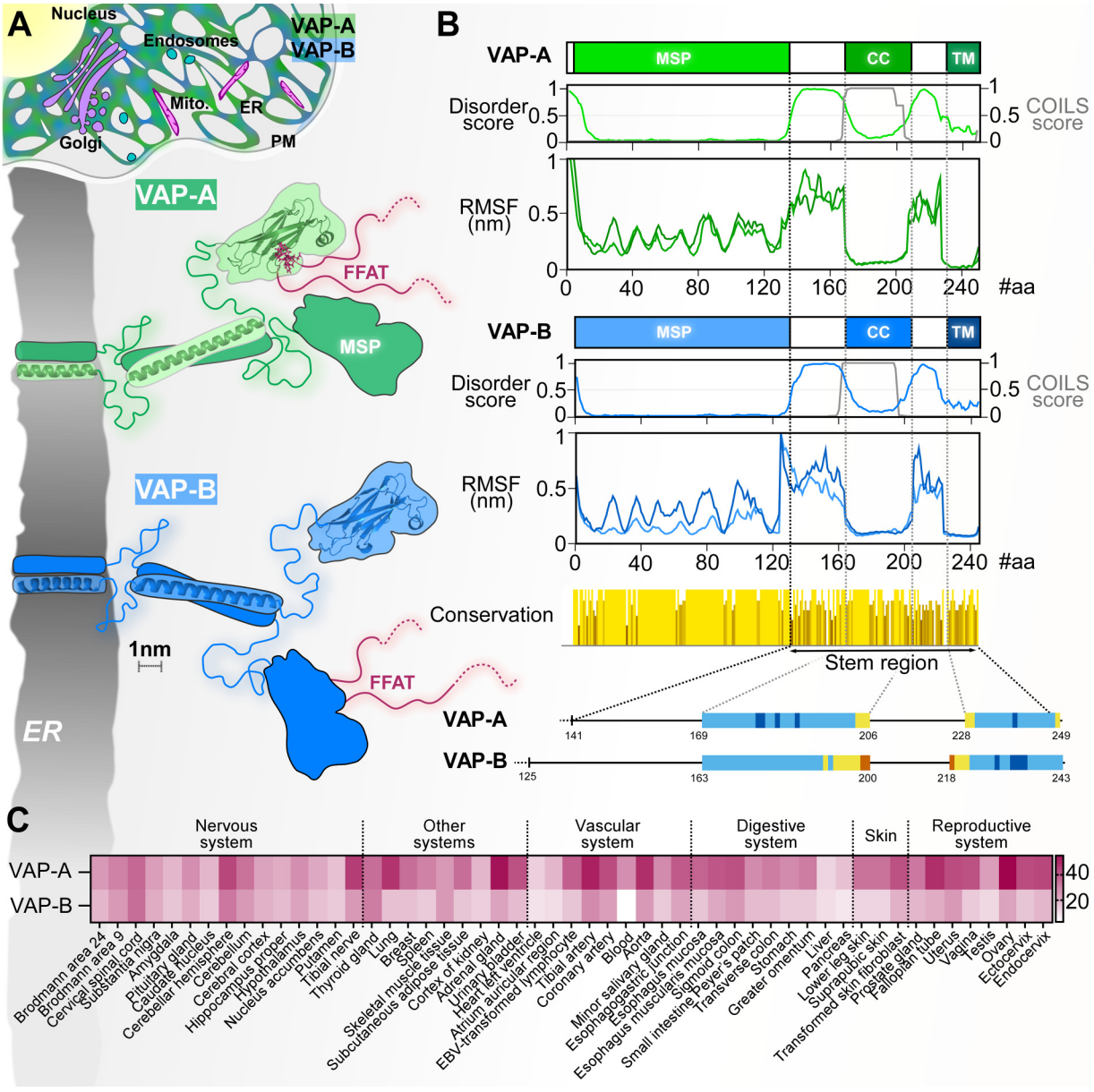

Figure 1. Similarities and differences between VAP-A and VAP-B. A: VAP-A and VAP-B have similar subcellular distribution and structural organization. B: The graphs show disorder prediction, coiled-coil probability score (grey line), and RMSF values calculated from MD simulations with full-length VAP-A or VAP-B having their TM helices inserted into a lipid bilayer. The two lines represent the RMSF of each monomer of a dimeric protein. Linker regions show larger fluctuation sizes. The conservation score (yellow scale) indicates that sequence divergence between VAP-A and VAP-B occurs primarily in the stem region. The helical structures of the VAP-A and VAP-B stem regions, as predicted by AlphaFold, are shown below. The color code shows the degree of confidence (high, dark blue; medium, light blue; low, yellow; very low, dark orange). C: Quantitative genetic expression of VAP-A and VAP-B among tissues, as determined by RNA sequencing, from the GTEx database (https://www.ebi.ac.uk/gxa/experiments/E-MTAB-5214). Expression levels in TPM (transcripts per million) are indicated according to the scale on the right.

can induce aggregate formation (Ratnaparkhi et al., 2008). Of note, MSP domains are also found in ER-resident mobile sperm domain-containing proteins (MOSPD1, 2 and 3), although MOSPD1 and MOSPD3 recognize motifs called "two phenylalanines in a neutral tract" (FFNT) (Cabukusta et al., 2020). MOSPD2 binds to FFAT motifs, but evidence suggests that it has distinct functions, notably via its CRAL-TRIO domain, and a lower abundance compared to VAP-A and VAP-B (Di Mattia et al., 2018; Zouiouich et al., 2022).

The interactomes of VAP-A and VAP-B (also called "VAPome") have been revealed using affinity

chromatography coupled to mass spectrometry (Huttlin et al., 2015), and proximity labeling approaches, either through BioID, which is based on proximity-dependent biotinylation of proteins by a biotin ligase fused to VAP (Cabukusta et al., 2020), or a modified ascorbate peroxidase 2 (APEX2) screen (James et al., 2019). These studies revealed new hits or confirmed known VAP-A and VAP-B interactors, such as OSBP and OSBP-related proteins, PTPIP51, CERT, VPS13A, MIGA2, PITPs and ACBD5, which are involved in lipid exchange at MCS, Rtn4, involved in membrane shaping, and sorting nexins (SNX), involved in membrane remodeling and transport (James and Kehlenbach, 2021). Of note, FFAT-containing proteins represent only ~50% of the identified putative VAP partners (Murphy and Levine, 2016), suggesting that VAP-mediated interactions are not limited to MSP-FFAT binding. Importantly, the VAP-A and VAP-B interactomes do not fully overlap, as a significant number of hits are listed as specific partners of VAP-A (such as ORP7, ZFPL1, and TMEM38B) or of VAP-B (such as SNX2, ACBD4, and Ric-8) (James and Kehlenbach, 2021). It is unclear, however, what predicts specificity for one or the other protein. Since the MSP domains of VAP-A and VAP-B are very similar, their "stem" regions (comprising linkers, coiled-coil, and TM domain), which show sequence divergence, may promote the formation of specific protein complexes. Such interactions that are independent of the MSP have been reported with different partners (Hamamoto et al., 2005; Saito et al., 2008; Amini-Bavil-Olyaee et al., 2013; Forrest et al., 2013). This is the case for the phosphatase Sac1, which exhibits a better affinity for VAP-A than VAP-B (Wakana et al., 2015). Another example is Protrudin, an ER-resident and FFAT-containing protein that regulates neurite formation and axonal regeneration (Saita et al., 2009; Petrova et al., 2020). Interestingly, Protrudin preferentially associates with VAP-A rather than VAP-B, recognizing not only its MSP domain but also its TM domain (Saita et al., 2009).

The stem region might also confer specific properties to VAP-A that differ from VAP-B, such as oligomerization, flexibility, membrane diffusion, and subcellular localization, which in turn would support association with some partners over others. VAP-A and VAP-B are considered dimeric proteins, mainly due to their coiled-coil region, which consists of six putative heptads that would form a rigid rod of 5.9 nm. The TM α-helices of VAP-A and VAP-B also contain a conserved dimerization GxxxG motif. However, there are conflicting data on the ability of TM domain alone to form dimers (Kim et al., 2010; Cabukusta et al., 2020). Some studies also report that VAP-A and VAP-B are capable of forming heterodimers, but it remains unclear to what extent this occurs (Nishimura et al., 1999; Kim et al., 2010; Cabukusta et al., 2020). What about the role of MSP in dimerization? In the crystal structure, the MSP domain of VAP-A forms a 2:2 complex with FFAT, where MSP domains resemble a flytrap sandwiching two FFAT (Kaiser et al., 2005). By contrast, in NMR studies, VAP-A MSP makes a 1:1 complex with the FFAT motif (Furuita et al., 2010), and no contribution of the MSP to the dimerization of VAP-B was reported (Kim et al., 2010). Nevertheless, future studies will be needed to define the stoichiometry between VAP-A or VAP-B and their partners, as many of them are also organized as dimers, and may occupy the same contact sites. It is also worth noting that chemical cross-linking analyses suggested the existence of other oligomeric forms for VAP-B (monomer, tetramer) (Kim et al., 2010), but their functional impact at the molecular and cellular level remains obscure. This is potentially important when considering the lateral diffusion of VAP along the ER membrane. It is known that the subcellular localization of VAP-A or VAP-B can be modulated upon overexpression of one of its partners. For example, overexpression of OSBP brings VAP-A to ER/Golgi MCS (Mesmin et al., 2013). Recent single particle tracking (sptPALM) analyzes revealed that the trajectory of VAP-B shows localization hubs that correspond to ER/mitochondria MCS (Obara et al., 2022). Indeed, the diffusion of VAP-B along the ER decreases from ~1.8 to ~0.25 $\mu m^2/s$ when engaged in a contact site. As expected, overexpression of its partner PTPIP51 concentrates VAP-B at MCS; but without its MSP, VAP-B randomly explores the entire surface of the ER. Interestingly, in the regions that encompasses the TM helix, AlphaFold predicts different α-helix lengths for VAP-A (20 residues) and VAP-B (24 residues) (Jumper et al., 2021; Varadi et al., 2021) (Figure 1B), although other prediction programs (TOPCONS, DeepTMHMM, MEMSAT-SVM, etc.) suggest more similar lengths (~19 residues on average). Of note, a mismatch between TM helix length and membrane thickness, which is largely determined by its lipid composition, can drive lateral and subcellular protein sorting (Levental and Lyman, 2023). For example, plasma membrane TM helices are on average longer than those of the ER and Golgi (the mean hydrophobic length is 20.3 residues in the ER and 24.4 in the plasma membrane) (Sharpe et al., 2010). Moreover, evidence suggests that proteins and lipids can co-segregate locally in the ER membrane, based on their biophysical properties, which may impact protein enrichment at MCS (Prasad et al., 2020; Zhemkov et al., 2021), and MCS organization (King et al., 2020). Thus, if TM helix lengths are different between VAP-A and VAP-B, they could mediate lateral segregation and/or adapt them to specific MCS.

Another structural feature worth mentioning is VAP linker regions, which show the most significant sequence variation between VAP-A and VAP-B. In a recent study, we demonstrated that these linkers are responsible for VAP-A flexibility, and are necessary for its engagement in the highly dynamic ER/Golgi MCS (Mora et al., 2021; Subra et al., 2023). By contrast, mutants of VAP-A designed to be more rigid only adapt to ER/Mitochondria MCS, which are more stable over time. Intrinsic disorder prediction suggests that VAP-B linkers are unstructured, similar to those of

VAP-A. In Figure 1B, we show original molecular dynamics (MD) simulation data of full-length VAP-A versus VAP-B inserted into membranes. The RMSF values clearly indicate a higher mobility of the amino acids present in the linkers, suggesting that like VAP-A, VAP-B has two very flexible regions flanking its coiled-coil domain. It should be noted that there is a less abundant, natural isoform of VAP-A produced by alternative splicing that differs from canonical VAP-A by the insertion of 45 residues in its first linker. Disorder prediction indicates that the inserted sequence is unstructured, thus forming an extra-long flexible linker 1. We have shown that expressing this isoform rescued a range of defects associated with ER/Golgi and ER/mitochondria MCS in VAP-A KO cells (Subra et al., 2023), but the functional implication of this splice variant remains to be determined. As a side note, there is also a splice variant of VAP-B, called VAP-C, whose sequence stops in the middle of the MSP, but its function remains largely unexplored.

A number of studies have demonstrated clear functional differences between VAP-A and VAP-B. For example, it has been shown that VAP-A, but not VAP-B, plays a key role with ORP3 and Rab7 in promoting the entry of lates endosomes in deep nuclear envelope invaginations that penetrate into the nucleoplasm, possibly by facilitating MCS formation between these compartments (Santos et al., 2018). By contrast, a specific function for VAP-B was shown in differentiated motor neurons: in these cells, VAP-B depletion alters phosphoinositide balance and significantly delays neurite extension (Genevini et al., 2019). In rescue experiments, neurogenesis levels recovered to control cells with VAP-B expression, but less so when using the corresponding VAP-A construct. In a recent study, we showed divergent implications of VAP-A and VAP-B on mitochondrial morphology and cardiolipin (CL) levels in hTERT-immortalized retinal pigment epithelial (RPE-1) cells. Our data indicated that knocking out VAP-A, but not VAP-B, results in decreased CL levels associated with defective mitochondrial fusion (Subra et al., 2023). Of note, RPE-1 cells have comparable levels of VAP-A and VAP-B, suggesting that functional differences exist between these proteins. In these cited studies, however, the underlying molecular basis for why one VAP is involved in a given function and not the other remains elusive. Nevertheless, unlike VAP-B, VAP-A KO is lethal at the embryonic stage in mice (Kabashi et al., 2013; McCune et al., 2017), implying that VAP-B is less important and/or less abundant than VAP-A, and further suggesting that VAP-A can replace VAP-B in its functions, but not vice versa. There is indeed a striking difference in the transcript levels of VAP-A and VAP-B genes between tissues and, as a general rule, VAP-B transcript levels are reduced compared to VAP-A (Figure 1C) (Consortium et al., 2015). Of note, they appear to be more balanced in the nervous system than in other tissues. Nevertheless, VAP-A was shown to be at least four times more abundant than VAP-B in mouse motoneuron-like cells (Genevini et al., 2019). Future studies will be necessary to define the molecular basis explaining the preferences of each of the VAPs for different partners, and thus the set of functions that are not shared between VAP-A and VAP-B, as their respective roles may diverge to varying degrees depending on the cell type or tissue considered.

Methods

MD Simulations of VAP-A and VAP-B Dimer Models

MD simulations were performed essentially as described previously (Subra et al., 2023), except that full-length membranous VAP-A and VAP-B proteins were simulated. Simulations of modified VAP-A and VAP-B structures from AlphaFold in a membrane were prepared with CHARMM-GUI using 560 POPC, 560 DOPC, and 56 cholesterol (5% cholesterol), a water thickness of 30 Å at a temperature of 303 K and neutralized with 120 mM NaCl. The TM domains were inserted into the membrane using the PPM 2.0 tool. Energy minimization and simulations were performed as described previously except that two NVT and four NPT equilibrations were performed using the Berendsen thermostat and barostat. Simulations (1 µs) were done in triplicate, using Gromacs 2021.3 (https://www.gromacs.org/) with the CHARMM36 force-field, and the TIP3P water model. MD analyzes of the root mean square fluctuation (RMSF) was performed as described previously (Subra et al., 2023).

Web Servers for Secondary Structure Prediction

For disorder prediction, we used DISOPRED3 (http://bioinf.cs.ucl.ac.uk/disopred). For the coiled-coil probability score, we used COILS (https://npsa-prabi.ibcp.fr/NPSA/npsa_lupas.html). For TM helix prediction, we used the following web servers: TOPCONS (https://topcons.cbr.su.se/), DeepTMHMM (https://dtu.biolib.com/DeepTMHMM/), MEMSAT-SVM (http://bioinf.cs.ucl.ac.uk/psipred/), HMMpTM (http://aias.biol.uoa.gr/HMMpTM/index.php) and CCTOP (https://cctop.ttk.hu/). Predictions from TOPCONS and CCTOP give consensus results from several algorithms.

Acknowledgments

We thank Amanda Patel (IPMC, Valbonne) for critical reading of the manuscript.

Declaration of Conflicting Interests

The authors declared no potential conflicts of interest with respect to the research, authorship, and/or publication of this article.

Funding

The authors disclosed receipt of the following financial support for the research, authorship, and/or publication of this article: Fondation pour la Recherche Médicale, Agence Nationale de la Recherche (grant number FDT202204015217, ANR-15-IDEX-01, ANR-21-CE13-0021-01), Polytech Nice Sophia (Université Côte d'Azur) PhD fellowship program.

ORCID iD

Bruno Mesmin https://orcid.org/0000-0002-5437-3246

References

Alpy F, Rousseau A, Schwab Y, et al. (2013). STARD3 or STARD3NL and VAP form a novel molecular tether between late endosomes and the ER. J Cell Sci *126*, 5500–5512. doi: 10.1242/jcs.139295

Amini-Bavil-Olyaee S, Choi YJ, Lee JH, et al. (2013). The antiviral effector IFITM3 disrupts intracellular cholesterol homeostasis to block viral entry. Cell Host Microbe *13*, 452–464. doi: 10.1016/j.chom.2013.03.006

Borgese N, Navone F, Nukina N, et al. (2021). Mutant VAPB: Culprit or innocent bystander of amyotrophic lateral sclerosis? Contact *4*, 25152564211022516. doi: 10.1177/25152564211022515

Cabukusta B, Berlin I, Elsland DM van, et al. (2020). Human VAPome analysis reveals MOSPD1 and MOSPD3 as membrane contact site proteins interacting with FFAT-related FFNT motifs. Cell Rep *33*, 108475. doi: 10.1016/j.celrep.2020.108475

Consortium TGte, Ardlie KG, Deluca DS, et al. (2015). The genotype-tissue expression (GTEx) pilot analysis: Multitissue gene regulation in humans. Science *348*, 648–660. doi: 10.1126/science.1262110

Di Mattia T, Martinet A, Ikhlef S, et al. (2020). FFAT Motif phosphorylation controls formation and lipid transfer function of inter-organelle contacts. EMBO J *39*(23), e104369. doi: 10.15252/embj.2019104369

Di Mattia T, Wilhelm LP, Ikhlef S, et al. (2018). Identification of MOSPD2, a novel scaffold for endoplasmic reticulum membrane contact sites. EMBO Rep *19*(7), e45453. doi: 10.15252/embr.201745453

Forrest S, Chai A, Sanhueza M, et al. (2013). Increased levels of phosphoinositides cause neurodegeneration in a Drosophila model of amyotrophic lateral sclerosis. Human Mol Genet *22*, 2689–2704. doi: 10.1093/hmg/ddt118

Furuita K, Jee J, Fukada H, et al. (2010). Electrostatic interaction between oxysterol-binding protein and VAMP-associated protein a revealed by NMR and mutagenesis studies. J Biol Chem *285*, 12961–12970. doi: 10.1074/jbc.m109.082602

Genevini P, Colombo MN, Venditti R, et al. (2019). VAPB Depletion alters neuritogenesis and phosphoinositide balance in motoneuron-like cells: Relevance to VAPB-linked amyotrophic lateral sclerosis. J Cell Sci *132*, jcs220061. doi: 10.1242/jcs.220061

Hamamoto I, Nishimura Y, Okamoto T, et al. (2005). Human VAP-B is involved in hepatitis C virus replication through interaction with NS5A and NS5B. J Virol *79*, 13473–13482. doi: 10.1128/jvi.79.21.13473-13482.2005

Huttlin EL, Ting L, Bruckner RJ, et al. (2015). The BioPlex network: A systematic exploration of the human interactome. Cell *162*, 425–440. doi: 10.1016/j.cell.2015.06.043

James C, Kehlenbach RH (2021). The interactome of the VAP family of proteins: An overview. Cells *10*, 1780. doi: 10.3390/cells10071780

James C, Müller M, Goldberg MW, et al. (2019). Proteomic mapping by rapamycin-dependent targeting of APEX2 identifies binding partners of VAPB at the inner nuclear membrane. J Biol Chem *294*, 16241–16254. doi: 10.1074/jbc.ra118.007283

Jumper J, Evans R, Pritzel A, et al. (2021). Highly accurate protein structure prediction with AlphaFold. Nature *596*, 583–589. doi: 10.1038/s41586-021-03819-2

Kabashi E, Oussini HE, Bercier V, et al. (2013). Investigating the contribution of VAPB/ALS8 loss of function in amyotrophic lateral sclerosis. Human Mol Genet *22*, 2350–2360. doi: 10.1093/hmg/ddt080

Kaiser SE, Brickner JH, Reilein AR, et al. (2005). Structural basis of FFAT motif-mediated ER targeting. Structure *13*, 1035–1045. doi: 10.1016/j.str.2005.04.010

Kim S, Leal SS, Halevy DB, et al. (2010). Structural requirements for VAP-B oligomerization and their implication in amyotrophic lateral sclerosis-associated VAP-B(P56S) Neurotoxicity. J Biol Chem *285*, 13839–13849. doi: 10.1074/jbc.m109.097345

King C, Sengupta P, Seo AY, et al. (2020). ER Membranes exhibit phase behavior at sites of organelle contact. Proc Nat Acad Sci *117*, 7225–7235. doi: 10.1073/pnas.1910854117

Kors S, Costello JL, Schrader M (2022). VAP Proteins – from organelle tethers to pathogenic host interactors and their role in neuronal disease. Front Cell Dev Biol *10*, 895856. doi: 10.3389/fcell.2022.895856

Levental I, Lyman E (2023). Regulation of membrane protein structure and function by their lipid nano-environment. Nat Rev Mol Cell Biol *24*, 107–122. doi: 10.1038/s41580-022-00524-4

Loewen CJR, Roy A, Levine TP (2003). A conserved ER targeting motif in three families of lipid binding proteins and in Opi1p binds VAP. EMBO J *22*, 2025–2035. doi: 10.1093/emboj/cdg201

McCune BT, Tang W, Lu J, et al. (2017). Noroviruses co-opt the function of host proteins VAPA and VAPB for replication via a phenylalanine–phenylalanine-acidic-tract-motif mimic in nonstructural viral protein NS1/2. mBio *8*, e00668-17. doi: 10.1128/mbio.00668-17

Mesmin B, Bigay J, Moser von Filseck J, et al. (2013). A four-step cycle driven by PI(4)P hydrolysis directs sterol/PI(4)P exchange by the ER-Golgi tether OSBP. Cell *155*, 830–843. doi: 10.1016/j.cell.2013.09.056

Mora E de la, Dezi M, Cicco AD, et al. (2021). Nanoscale architecture of a VAP-A-OSBP tethering complex at membrane contact sites. Nat Commun *12*, 3459. doi: 10.1038/s41467-021-23799-1

Murphy SE, Levine TP (2016). VAP, a versatile access point for the endoplasmic reticulum: Review and analysis of FFAT-like motifs in the VAPome. Biochim Biophys Acta Mol Cell Biol Lipids *1861*, 952–961. doi: 10.1016/j.bbalip.2016.02.009

Nakamichi S, Yamanaka K, Suzuki M, et al. (2011). Human VAPA and the yeast VAP Scs2p with an altered proline distribution can phenocopy amyotrophic lateral sclerosis-associated VAPB (P56S). Biochem Biophys Res Commun *404*, 605–609. doi: 10.1016/j.bbrc.2010.12.011

Neefjes J, Cabukusta B (2021). What the VAP: The expanded VAP family of proteins interacting with FFAT and FFAT-related motifs for interorganellar contact. Contact *4*, 251525642110122. doi: 10.1177/25152564211012246

Nishimura AL, Mitne-Neto M, Silva HCA, et al. (2004). A mutation in the vesicle-trafficking protein VAPB causes late-onset spinal muscular atrophy and amyotrophic lateral sclerosis. Am J Human Genet *75*, 822–831. doi: 10.1086/425287

Nishimura Y, Hayashi M, Inada H, et al. (1999). Molecular cloning and characterization of mammalian homologues of vesicle-associated membrane protein-associated (VAMP-associated) proteins. Biochem Biophys Res Commun *254*, 21–26. doi: 10.1006/bbrc.1998.9876

Obara CJ, Nixon-Abell J, Moore AS, et al. (2022). Motion of single molecular tethers reveals dynamic subdomains at ER-mitochondria contact sites. *bioRxiv*. 2022.09.03.505525. doi: 10.1101/2022.09.03.505525

Petrova V, Pearson CS, Ching J, et al. (2020). Protrudin functions from the endoplasmic reticulum to support axon regeneration in the adult CNS. Nat Commun *11*, 5614. doi: 10.1038/s41467-020-19436-y

Prasad R, Sliwa-Gonzalez A, Barral Y (2020) Mapping bilayer thickness in the ER membrane. Sci Adv *6*, eaba5130. doi: 10.1126/sciadv.aba5130

Ratnaparkhi A, Lawless GM, Schweizer FE, et al. (2008). A drosophila model of ALS: Human ALS-associated mutation in VAP33A suggests a dominant negative mechanism. PLoS One *3*, e2334. doi: 10.1371/journal.pone.0002334

Saita S, Shirane M, Natume T, et al. (2009). Promotion of neurite extension by protrudin requires its interaction with vesicle-associated membrane protein-associated protein. J Biol Chem *284*, 13766–13777. doi: 10.1074/jbc.m807938200

Saito S, Matsui H, Kawano M, et al. (2008). Protein phosphatase 2Cε is an endoplasmic reticulum integral membrane protein that dephosphorylates the ceramide transport protein CERT to enhance its association with organelle membranes. J Biol Chem *283*, 6584–6593. doi: 10.1074/jbc.m707691200

Santos MF, Rappa G, Karbanová J, et al. (2018). VAMP-associated protein-A and oxysterol-binding protein–related protein 3 promote the entry of late endosomes into the nucleoplasmic reticulum. J Biol Chem *293*, 13834–13848. doi: 10.1074/jbc.ra118.003725

Sharpe HJ, Stevens TJ, Munro S (2010). A comprehensive comparison of transmembrane domains reveals organelle-specific properties. Cell *142*, 158–169. doi: 10.1016/j.cell.2010.05.037

Subra M, Dezi M, Bigay J, et al. (2023). VAP-A intrinsically disordered regions enable versatile tethering at membrane contact sites. Dev Cell *58*, 121–138.e9. doi: 10.1016/j.devcel.2022.12.010

Sun EW, De Camilli P (2018). Kv2 potassium channels meet VAP. Proc Nat Acad Sci *115*, 7849–7851. doi: 10.1073/pnas.1810059115

Varadi M, Anyango S, Deshpande M, et al. (2021). Alphafold protein structure database: Massively expanding the structural coverage of protein-sequence space with high-accuracy models. Nucleic Acids Res *50*, D439–D444. doi: 10.1093/nar/gkab1061

Wakana Y, Kotake R, Oyama N, et al. (2015). CARTS Biogenesis requires VAP–lipid transfer protein complexes functioning at the endoplasmic reticulum–Golgi interface. Mol Biol Cell *26*, 4686–4699. doi: 10.1091/mbc.e15-08-0599

Xu L, Wang X, Zhou J, et al. (2020). Miga-mediated endoplasmic reticulum–mitochondria contact sites regulate neuronal homeostasis. eLife *9*, e56584. doi: 10.7554/elife.56584

Yeo HK, Park TH, Kim HY, et al. (2021). Phospholipid transfer function of PTPIP51 at mitochondria-associated ER membranes. EMBO Rep *22*, e51323. doi: 10.15252/embr.202051323

Zhemkov V, Ditlev JA, Lee W-R, et al. (2021). The role of Sigma 1 receptor in organization of endoplasmic reticulum signaling microdomains. eLife *10*, e65192. doi: 10.7554/elife.65192

Zouiouich M, Di Mattia T, Martinet A, et al. (2022). MOSPD2 Is an endoplasmic reticulum–lipid droplet tether functioning in LD homeostasis. J Cell Biol *221*, e202110044. doi: 10.1083/jcb.202110044